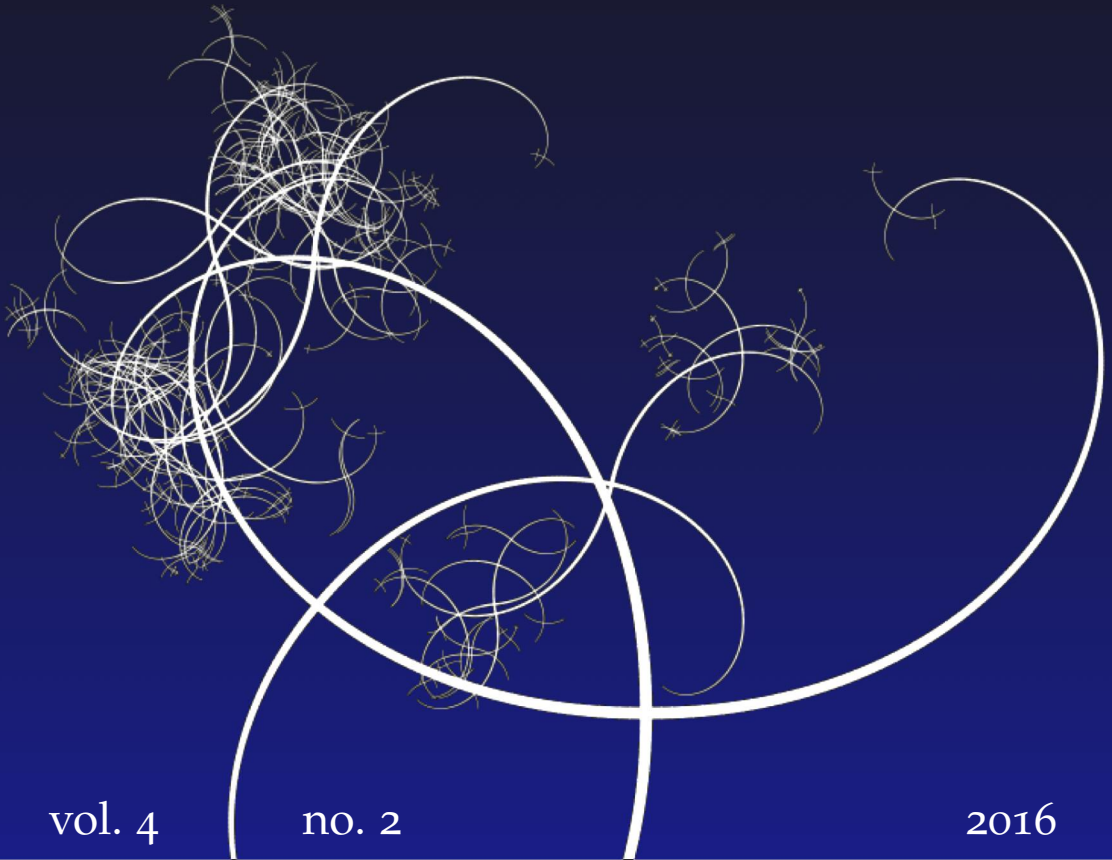


NISSUNA UMANA INVESTIGAZIONE SI PUO DIMANDARE VERA SCIENZA
S'ESSA NON PASSA PER LE MATEMATICHE DIMOSTRAZIONI
LEONARDO DA VINCI



vol. 4

no. 2

2016

MATHEMATICS AND MECHANICS
of
Complex Systems

MICKHAIL A. GUZEV AND ALEXANDR A. DMITRIEV

STABILITY ANALYSIS OF TWO COUPLED OSCILLATORS





STABILITY ANALYSIS OF TWO COUPLED OSCILLATORS

MICKHAIL A. GUZEV AND ALEXANDR A. DMITRIEV

We study a system of two coupled oscillators linked by a linear elastic spring and positioned vertically in a uniform gravity field. It is demonstrated that the system has different equilibrium configurations below and above the oscillators' suspension centers. We obtained the relations of the string stiffness and the distance between the suspension centers identifying the stability region of the oscillators.

1. Introduction

Mechanical oscillators are models of various physical processes and complex physical systems as demonstrated by a vast body of literature. For example, coupled oscillators are used to describe the lattice vibrations in crystals [Kittel 2005].

A well-known and useful oscillator system is the sympathetic oscillators [Sommerfeld 1994], which are two linked oscillators with equal rods and masses interacting through a spring. Small linear oscillations about the equilibrium point have been studied, focusing on analyzing the physical situations depending on the spring stiffness.

There have been many scientific studies on oscillating dynamics of mechanical systems. However, new results still periodically appear. For instance, Maianti et al. [2009] study the impact of symmetrical initial conditions of linked oscillators in a uniform gravity field on the eigenoscillations and obtain the initial angle that ensures an independent frequency spectrum. Ramachandran et al. [2011] deal with different configurations of two pendulums connected by a rod. The results are that there are stable equilibrium configurations that are asymmetrical with respect to the vertical midline. An important property of the system is that there can appear bifurcations depending on the distance between the suspension points. The obtained results are useful for investigation of the pantographic structures [dell'Isola et al. 2016]. The interest in these materials is defined by development of the three-dimensional printing technology. They can be regarded as families of pendulums (also called fibers) interconnected by pivots in equilibrium. Synchronization of

Communicated by Francesco dell'Isola.

MSC2010: 70E55, 70H14.

Keywords: coupled oscillators, equilibrium configurations, stability, linear interaction.

two oscillators is the focus of [Koluda et al. 2014] and their chaotic dynamics is studied in [Huynh and Chew 2010; Huynh et al. 2013].

A system of inverted oscillators also provides physically sound phenomena. Stable positions can also be attained if there is a fast perturbation frequency [Stephenson 1908]. This result is due to Pyotr Kapitza [Kapitza 1951a; Kapitza 1951b]. A more accurate condition of dynamical stabilization of an inverted oscillator is introduced in [Butikov 2011]. Chelomei's problem of the stabilization of an elastic, statically unstable rod by means of a vibration is considered in [Seyranian and Seyranian 2008]. The stability of two inverted linearly linked oscillators is analyzed in [Markeev 2013]. The author reveals bifurcations depending on the linking spring stiffness and single out parameters that lead to stable or unstable equilibria. The phenomenon of stabilization by parametric excitation of an elastically restrained double inverted pendulum is considered in [Arkhipova et al. 2012]. The problem of restabilization of statically unstable linear Hamiltonian systems is analyzed in [Arkhipova and Luongo 2014]. A comprehensive review of the dynamics of a large number of coupled oscillators is presented in [Pikovsky and Rosenblum 2015].

The objective of the current paper is to study the stability of the model of two linearly interacting oscillators in a uniform gravity field. The formal analysis of equilibrium stability is carried out in the framework of the linear stability approach. It consists of determination of the equilibrium position and calculation of the matrix of the second partial derivatives of potential energy in the equilibrium position. If the matrix spectrum is positive, the equilibrium is stable. Otherwise, it is unstable. We focus on analyzing the equilibrium solutions depending on the distance between the suspension points and the spring stiffness. This analysis includes different configurations of the model of coupled oscillators.

2. Basic equations

Let us consider two oscillators of length l and mass m in a uniform gravity field. We assume that the suspension points O_1 and O_2 are positioned on a motionless horizontal straight line, while the distance between the suspension points a is constant. A massless elastic spring of stiffness k links the masses at points B_1 and B_2 , which coincide with the masses' positions. We assume that the oscillators move in a fixed vertical plane containing the interval $O_1 O_2$ (see Figure 1). The oscillators can be situated both below the horizontal suspension line (see the region A1 in Figure 1, left) and above it (see the region A2 in Figure 1, right). In the region A1, angles φ_1 and φ_2 lie in the interval $(0, \pi)$, while transition to the region A2 implies the transformation $\varphi_1, \varphi_2 \mapsto -\varphi_1, -\varphi_2$.

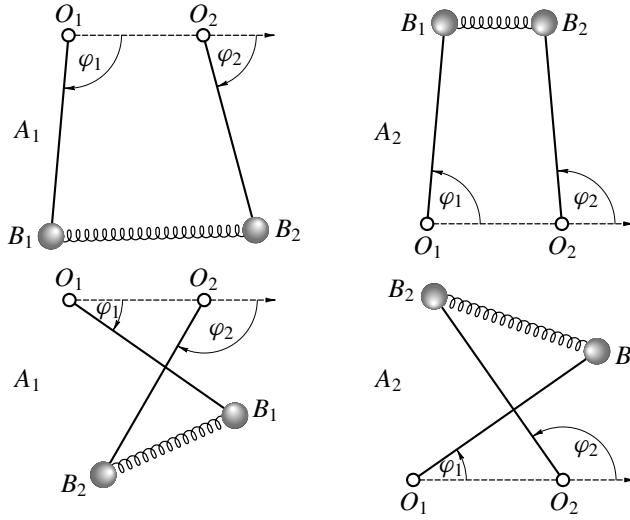


Figure 1. Top left: the classical configuration and the region A1. Top right: the classical configuration and the region A2. Bottom left: the modified configuration and the region A1. Bottom right: the modified configuration and the region A2.

Hence, in this article, we consider different configurations of the oscillator model. Configurations presented in Figure 1, top left, correspond to the sympathetic oscillators [Sommerfeld 1994], and configurations of Figure 1, top right, describe a system of inverted oscillators. Both models are well-known in scientific literature, so configurations presented in Figure 1, top, will be called the classical ones.

Configurations of Figure 1, bottom, are presented in [Ramachandran et al. 2011] (called “modified configurations” to distinguish them from Figure 1, top).

It is clear that the kinetic energy of the oscillators is

$$T = \frac{ml^2}{2} [(\dot{\varphi}_1)^2 + (\dot{\varphi}_2)^2]. \quad (1)$$

Potential energy U includes the energy of the oscillator interaction $k(d-a)^2/2$ and the gravity field energy where d is the spring length. In the region A1, oscillators linked by a linear elastic spring provide

$$U = U(\varphi_1, \varphi_2) = \frac{k(d-a)^2}{2} - mgl(\sin \varphi_1 + \sin \varphi_2) \quad (2)$$

while in the region A2 there is a transformation $g \mapsto -g$ in (2). In the regions A1 and A2, the spring length is given by the formula

$$d = \sqrt{[a + l(\cos \varphi_2 - \cos \varphi_1)]^2 + l^2(\sin \varphi_2 - \sin \varphi_1)^2}.$$

It is interesting that there is a natural geometrical condition for the configurations. In the case of the classical configurations (Figure 1, top), the difference of the rod length projections on the suspension axis is less than a , giving the condition

$$l(\cos \varphi_1 - \cos \varphi_2) < a. \quad (3)$$

In the case of the modified configurations (Figure 1, bottom), the corresponding difference is larger than a :

$$l(\cos \varphi_1 - \cos \varphi_2) > a. \quad (4)$$

From (1) and (2), the Lagrangian of the system ensures

$$L = T - U = \frac{ml^2}{2}(\dot{\varphi}_1^2 + \dot{\varphi}_2^2) - \frac{k(d-a)^2}{2} + 2mgl \sin \frac{\varphi_1 + \varphi_2}{2} \cos \frac{\varphi_1 - \varphi_2}{2}. \quad (5)$$

Now let us introduce instead of φ_1 and φ_2 new coordinates q_1 and q_2 , where $q_1 = (\pi - \varphi_1 - \varphi_2)/2$ and $q_2 = (\varphi_1 - \varphi_2)/2$. Introducing new dimensionless time $\tau = t\sqrt{2g/l}$ and Lagrangian $\Lambda = L/mgl$, (5) can be rewritten as

$$\begin{aligned} \Lambda &= \frac{1}{2}(\dot{q}_1^2 + \dot{q}_2^2) - \Pi(q_1, q_2), \\ \Pi &= \Pi(q_1, q_2) = \frac{(s - \mu)^2}{2\nu} - \cos q_1 \cos q_2, \\ s^2 &= \sin^2 q_2 + 2\mu \cos q_1 \sin q_2 + \mu^2, \quad \mu = \frac{a}{2l}, \quad \nu = \frac{2mgl}{k}. \end{aligned} \quad (6)$$

Parameter ν characterizes the relation between the potential energy of the oscillators and the spring's effective energy, while μ is a kinematic parameter and depends on the metric characteristics.

Differential equations of the oscillator dynamics in the form of Lagrangian equations are

$$\frac{d}{d\tau} \frac{\partial \Lambda}{\partial \dot{q}_i} = \frac{\partial \Lambda}{\partial q_i} \iff \ddot{q}_i = -\frac{\partial \Pi}{\partial q_i}, \quad i = 1, 2. \quad (7)$$

System (7) allows for solutions corresponding to both the classical and the modified configurations. Therefore, while analyzing system (7), it is necessary to point out the region of feasible solutions. Conditions (3)–(4) can be written as

$$\mu + \cos q_1 \sin q_2 > 0, \quad (8)$$

$$\mu + \cos q_1 \sin q_2 < 0. \quad (9)$$

Equilibrium configurations of the oscillator system ensue from the condition $\ddot{q}_i = 0$; then it follows from (7) that they are determined as the critical points of the system's potential energy

$$\frac{\partial \Pi}{\partial q_1} = 0, \quad \frac{\partial \Pi}{\partial q_2} = 0. \quad (10)$$

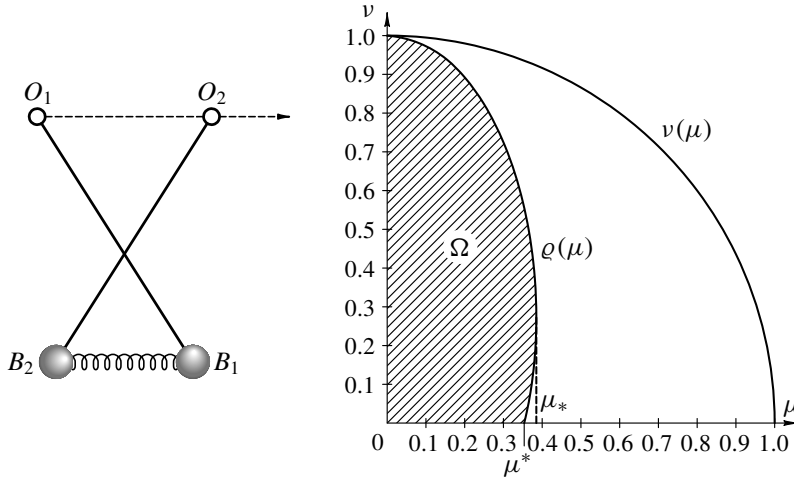


Figure 2. Left: the modified symmetric equilibrium configuration for the oscillator model in the region A1. Right: the stability domain Ω for the modified configuration in the region A1.

Taking into account (6), one can rewrite (10) in the form

$$\sin q_1 \left[\left(\frac{\mu}{s} - 1 \right) \mu \sin q_2 + \nu \cos q_2 \right] = 0, \quad (11)$$

$$\left(1 - \frac{\mu}{s} \right) (\sin q_2 + \mu \cos q_1) \cos q_2 + \nu \cos q_1 \sin q_2 = 0. \quad (12)$$

Thus, by solving the system (11)–(12), one obtains a set of equilibrium configurations.

3. Symmetrical equilibrium configurations

Symmetrical configurations are characterized by symmetrical positions of the pendulums with respect to the vertical midline. The classical symmetric configurations in the region A1 follow from $q_1 = 0$, while in the region A2 from $q_1 = \pi$. In this case, (11) is satisfied identically ($\sin q_1 = 0$); then the distance (6) between the oscillators equals $s = |\sin q_2 \pm \mu|$ and the condition (8) is equivalent to $\mu \pm \sin q_2 > 0$, i.e., $s = \mu \pm \sin q_2$. So (12) reduces to $\sin q_2 (\cos q_2 \pm \nu) = 0$, which was studied in [Markeev 2013].

The modified symmetrical configurations in the region A1 follow from $\varphi_2 = \pi - \varphi_1$, $q_1 = 0$, and are shown in Figure 2. This allows us to rewrite the condition (9) as $\mu + \sin q_2 < 0$, i.e., $\mu < 1$ and $|q_2| < \pi/2$; then the distance $s = -(\mu + \sin q_2)$ and (12) is equivalent to

$$\begin{aligned} (2\mu + \sin q_2) \cos q_2 + \nu \sin q_2 &= 0 \\ \iff \sin 2q_2 + 2\sqrt{4\mu^2 + \nu^2} \sin(q_2 - q^*) &= 0, \quad (13) \end{aligned}$$

where $q^* = -\arcsin(2\mu/\sqrt{4\mu^2 + \nu^2})$. Let $q^{**} = -\arcsin \mu$; then inside the interval (q^*, q^{**}) , (13) has a unique solution \tilde{q} provided the inequality

$$\nu < \sqrt{1 - \mu^2}, \quad \mu < 1, \quad (14)$$

is true. Indeed, (13) is identical to

$$2\mu + \sin q_2 = -\nu \tan q_2. \quad (15)$$

The right-hand side of (15) decreases; it equals $2\mu/\nu$ at point q^* and $\mu/\sqrt{1 - \mu^2}$ at point q^{**} . The left-hand side increases; it is less than $2\mu/\nu$ at point q^* and equals $2\mu/\nu$ at point q^{**} . If the inequality (14) is satisfied, the function graphs intersect at one and only one point \tilde{q} .

Let us analyze the type of equilibrium. The matrix of the second partial derivatives of potential Π at critical point $(0, \tilde{q})$ agrees with

$$\begin{aligned} \Pi_{11} &= \frac{\partial^2 \Pi}{\partial q_1^2} = \left(\frac{\mu}{s} - 1\right) \frac{\mu}{\nu} \sin \tilde{q} + \cos \tilde{q}, \\ \Pi_{22} &= \frac{\partial^2 \Pi}{\partial q_2^2} = \frac{1}{\nu} \left[\cos^2 \tilde{q} + \left(\frac{\mu}{s} - 1\right) (\sin \tilde{q} + \mu) \sin \tilde{q} \right] + \cos \tilde{q}, \\ \Pi_{12} &= \frac{\partial^2 \Pi}{\partial q_1 \partial q_2} = 0; \end{aligned}$$

i.e., the matrix is diagonal. At point \tilde{q} , since $s = -(\mu + \sin \tilde{q})$, (13) is equivalent to $(s - \mu) = \nu \tan \tilde{q}$, which results in

$$\Pi_{11} = \frac{\mu + \cos^2 \tilde{q} \sin \tilde{q}}{\cos \tilde{q} (\mu + \sin \tilde{q})}, \quad \Pi_{22} = \frac{1}{\nu} \cos^2 \tilde{q} + \frac{1}{\cos \tilde{q}}. \quad (16)$$

It is straightforward that $\Pi_{22} > 0$ and $\Pi_{11} > 0$ if

$$\mu + \cos^2 \tilde{q} \sin \tilde{q} < 0. \quad (17)$$

To solve (17), one needs to find the roots of the cubic parabola $x^3 - x - \mu$ as $x = \sin \tilde{q}$. It ensures the restrictions on parameter μ

$$0 < \mu < \mu_* = \frac{2}{3\sqrt{3}}, \quad x_1(\mu) < \sin \tilde{q} < x_2(\mu), \quad (18)$$

where $x_1(\mu)$ and $x_2(\mu)$ are the cubic parabola's roots:

$$\begin{aligned} x_1(\mu) &= -\frac{2}{\sqrt{3}} \sin\left(\frac{\pi}{6} + \phi(\mu)\right), \\ x_2(\mu) &= -\frac{2}{\sqrt{3}} \sin\left(\frac{\pi}{6} - \phi(\mu)\right), \end{aligned} \quad \phi(\mu) = \frac{1}{3} \arccos\left(\frac{\mu}{\mu_*}\right). \quad (19)$$

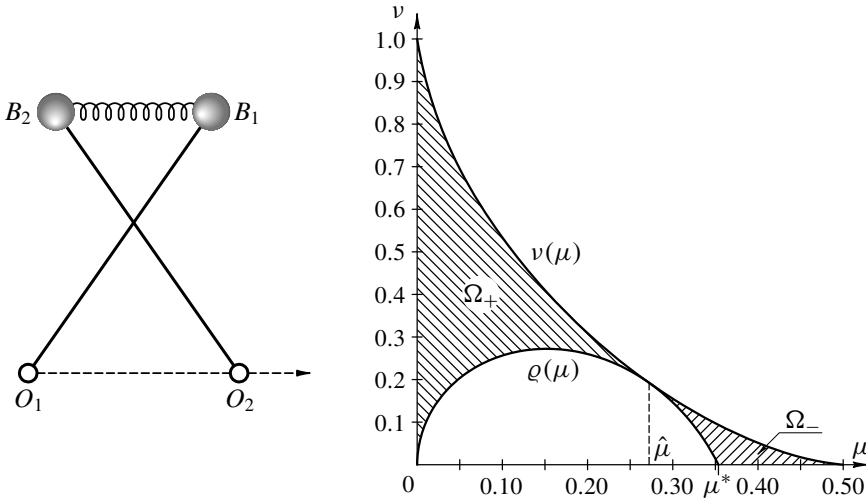


Figure 3. Left: the modified symmetric equilibrium configuration in the region A2. Right: the solution existence domain for the modified symmetric equilibrium configuration in the region A2. The region Ω_- is the stability region.

Thus, the oscillator model in the region A1 given the condition (14) has modified equilibrium configurations depending on the solution \tilde{q} of (13). This equilibrium is stable if the conditions (18) and (19) are satisfied.

Figure 2 shows that the region of solution existence is bounded by a circular arc $\nu(\mu) = \sqrt{1 - \mu^2}$. The shaded region Ω indicates parameters (μ, ν) that ensure stable configuration. The boundary of the stability region $\varrho(\mu)$ is determined by $\Pi_{11} = 0$. However, this formula is rather cumbersome; thus, it is not presented. It should be noted that $\varrho(\mu)$ has two branches merging at point μ_* .

If a point (μ, ν) is outside the domain Ω , then the critical point corresponding to the solution \tilde{q} of (13) is a saddle.

For the modified oscillator model, the equilibrium configurations in the region A2 follow from $q_1 = \pi$ ($\varphi_1 + \varphi_2 = -\pi$), the distance $s = \sin q_2 - \mu > 0$, i.e., $q_2 > 0$, and (12) takes the form

$$\sin q_2 = 2\mu + \nu \tan q_2. \tag{20}$$

The oscillator position corresponding to the region A2 is depicted in Figure 3.

Since $\sin q$ is a concave function as $q \in (0, \pi/2)$ and $\tan q$ is convex, the number of solutions of (20) depends on the parameters (μ, ν) . Particularly, q_0 exists if the function graphs have a common tangent, i.e., $\cos q_0 = \nu / \cos^2 q_0$. Substituting the obtained ν into (20), we get $2\mu = \sin^3 q_0$. It follows that there is a curve

$$\nu(\mu) = [1 - (2\mu)^{2/3}]^{3/2}, \tag{21}$$

whose points determine the only solution $q_0(\mu) = \arcsin(2\mu)^{1/3}$ of (20). The solution $q_0(\mu)$ is a bifurcation point. If one slightly varies the parameters (μ, ν) , (20) has either no solution or two solutions q_- and q_+ ($q_- < q_0(\mu) < q_+$). From convexity of $\tan q$, concavity of $\sin q$, and (21), it follows that the condition for two solutions is

$$\nu < [1 - (2\mu)^{2/3}]^{3/2},$$

which leads to $\mu < \frac{1}{2}$.

By analogy to (16), one can infer that

$$\Pi_{11} = \frac{\mu - \cos^2 q_{\pm} \sin q_{\pm}}{\cos q_{\pm}(\mu - \sin q_{\pm})}, \quad \Pi_{22} = \cos^2 q_{\pm} - \frac{\nu}{\cos q_{\pm}}.$$

The function $1 - \nu/\cos^3 q$ decreases and equals zero at $q_0(\mu)$; therefore, $\Pi_{22} < 0$ at the root q_+ of (20). Hence, the oscillators are unstable around the equilibrium from q_+ .

The value of Π_{11} is positive in the region where $h(q) = \mu - \cos^2 q \sin q$ is positive. This region ensures that

$$\sin q < x_1(\mu), \quad x_2(\mu) < \sin q, \quad 0 < \mu < \mu_*.$$

Figure 3 shows a shaded region Ω_+ , where $\Pi_{11} < 0$ at q_+ , and another shaded region Ω_- , where $\Pi_{11} > 0$ at q_- . The point $\hat{\mu}$ is a tangential point of curves $\nu(\mu)$ and $\varrho(\mu)$. Calculated values of $\hat{\mu} \approx 0.272166$ and $\hat{\nu} \approx 0.19245$.

Thus, in the region A2, the equilibria of the modified configurations are determined by the two solutions q_- and q_+ of (20), which exist as the parameters (μ, ν) comply with (21).

If the parameters (μ, ν) are inside the region Ω_+ , the critical point corresponding to q_+ is a maximum, while otherwise it is a saddle.

If the parameters (μ, ν) are inside the region Ω_- , the critical point corresponding to q_- is stable, while otherwise it is again a saddle.

4. Asymmetric equilibrium configurations

To study the asymmetric equilibria, it is convenient to use the variables $x = \sin q_2$ and $y = \cos q_1$. Since $-\pi/2 < q_2 < \pi/2$ and $0 < q_1 < \pi/2$ in the region A1 and $-\pi/2 < q_1 < 0$ in the region A2, these transformations result in a one-to-one mapping in each of the considered regions. It is straightforward that the variables x and y vary within the triangle $\Delta_+ = \{(x, y) : -1 < x < 1, 0 < y < 1\}$ in the region A1 and $\Delta_- = \{(x, y) : -1 < x < 1, -1 < y < 0\}$ in the region A2. Using the variables x and y , the potential Π is given by

$$\Pi(x, y) = \frac{(s - \mu)^2}{2\nu} \mp \sqrt{1 - x^2} \cdot y, \quad s^2 = x^2 + 2\mu xy + \mu^2,$$

where the minus corresponds to the region A1 and the plus corresponds to A2. Then the system (10) can be rewritten as

$$\begin{aligned} \mu \frac{s - \mu}{s} k(x) \mp v &= 0, \\ \frac{s - \mu}{s} (x + \mu y) \pm vk(x)y &= 0, \end{aligned} \quad k(x) = \frac{x}{\sqrt{1 - x^2}}.$$

By eliminating $(s - \mu)/s$, we obtain the relation $\mu y + x(1 - x^2) = 0$, which suggests that the critical points of the potential Π are determined from the system

$$h(x, \mu) = \mu \frac{s - \mu}{s} k(x) = \pm v, \tag{22}$$

$$\mu y + x(1 - x^2) = 0. \tag{23}$$

The left-hand side of (23) differs from the cubic parabola pertaining to (17), by a multiplier y at μ .

Substituting (23) in the s relation, one obtains

$$s^2 = 2x^4 - x^2 + \mu^2. \tag{24}$$

The triangle Δ_+ intersects the cubic parabola of (23) if

$$\begin{aligned} -\sqrt{1 - \mu} \leq x \leq x_1(\mu), & \quad \text{as } 0 < \mu < \mu_*, \\ x_2(\mu) \leq x \leq 0 & \\ -\sqrt{1 - \mu} \leq x \leq 0 & \quad \text{as } \mu_* \leq \mu < 1. \end{aligned} \tag{25}$$

Thus, *the asymmetric equilibria in the region A1 may exist only if $0 < \mu < 1$ and are determined by the solutions \tilde{x} of (22) as the s follows from (24) agreeing with (25).*

Condition (8) for the classical configurations takes the form

$$\mu + xy > 0. \tag{26}$$

Inequality (26) then can be rewritten as

$$x^2 + y^2 < 1, \quad y \geq -x \quad \text{as } -1 < x \leq 0. \tag{27}$$

Indeed, since $y < 0$ and $x < 0$, by multiplying (26) by y and using (23), we get

$$y(\mu + xy) = x(x^2 - 1) + xy^2 = x(x^2 + y^2 - 1) \geq 0 \quad \text{or} \quad x^2 + y^2 \leq 1.$$

For the modified configurations, the inequality sign in (26) changes to the opposite; then the condition of existence is determined by

$$x^2 + y^2 > 1, \quad y \geq -x \quad \text{as } -1 < x \leq 0. \tag{28}$$

On the other hand, by multiplying (26) by μ , one can determine the boundary demarcating the classical configuration from the modified one:

$$\mu^2 - x^2(1 - x^2) = 0.$$

By solving the biquadratic equation, one can find the intersection points of a unit circle and the cubic parabola of (23):

$$\hat{x}_1(\mu) = -\sqrt{\frac{1}{2} + \sqrt{\frac{1}{4} - \mu^2}}, \quad \hat{x}_2(\mu) = -\sqrt{\frac{1}{2} - \sqrt{\frac{1}{4} - \mu^2}}.$$

The asymmetric equilibrium is stable if the eigenvalues of the second derivative matrix of the potential Π are positive. It can be shown that the eigenvalues are positive if and only if $\det \Pi'' > 0$. Moreover, $\det \Pi''$ coincides with the accuracy of a multiplier with the derivative of $h(x, \mu)$ over x , which leads to

$$\det \Pi'' = \frac{\mu}{-x} h'(x, \mu).$$

By figuring out $h'(x, \mu)$ and omitting always-positive multipliers, one can see that the equilibrium is stable at the point \tilde{x} , the solution of (23), if the function

$$\Lambda(x, \mu) = \mu x^2(4x^2 - 1)(1 - x^2) + s^2(s - \mu)$$

is positive.

The stability region boundary is determined by $h(x, \mu) = v$ and $h'(x, \mu) = 0$. However, the condition $h'(x, \mu) = 0$ implies that the solution \tilde{x} is a local extremum of the function $h(x, \mu)$ and a bifurcation point of the solution of (22), which results in the solution \tilde{x} dividing into the two solutions $\tilde{x}_- < \tilde{x}_+$. One of the solutions is stable since $h'(x, \mu)$ changes its sign at the point \tilde{x} . The solutions of $\Lambda(x, \mu) = 0$ taking into account the corresponding restrictions on x determine x as a function of μ . Then by substituting it into (22), we have the function $\varrho(\mu)$, whose graph is the boundary of the stability region of the asymmetric equilibria.

The region A1. Equation (22) is written in the form

$$\mu \frac{s - \mu}{s} k(x) = v. \tag{29}$$

Since $k(x) < 0$, the function $h(x, \mu)$ is positive if $s < \mu$. This inequality is valid if $x^* = 1/\sqrt{2} < x < 0$. From this, it follows that in the region A1 the solution of (23) lies within the intersection of the interval $(x^*, 0)$ and the intervals determined by the inequalities (25).

In the case of classical configuration, the inequality (27) must be satisfied, while the modified configuration is valid given the inequality (28). The boundary of the solution existence region is determined by the maximal and minimal values of $h(x, \mu)$ for corresponding μ . The stability region is determined by the values

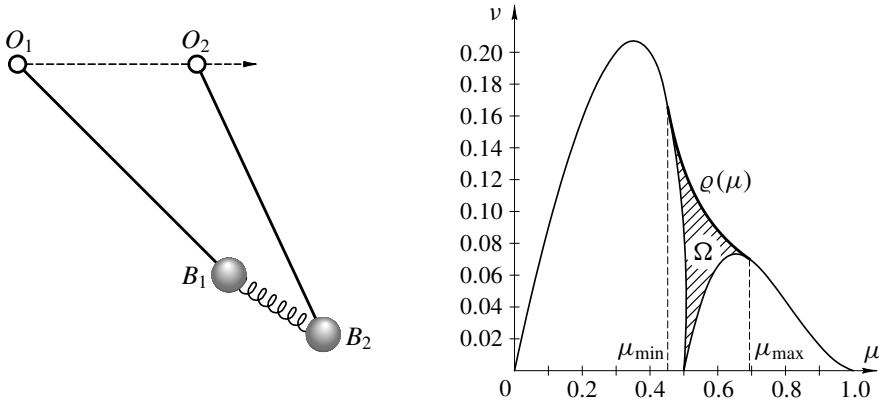


Figure 4. Left: the asymmetric classical configuration in the region A1. Right: the stability domain Ω of the asymmetric classical configuration in the region A1.

of $\varrho(\mu)$ while $\Lambda(x, \mu)$ must be positive. Figure 4, right, shows the solution existence region of (29) for the sympathetic oscillators (Figure 4, left). The values μ_{\min} and μ_{\max} are determined by the condition of maximality and minimality of μ , which ensures $\Lambda(x, \mu)$ to be zero. Calculated values of $\mu_{\min} \approx 0.452258$ and $\mu_{\max} \approx 0.693692$. The stable equilibrium region Ω is shaded and coincides with the region of two-solution existence $\tilde{x}_- < \tilde{x}_+$ of (22) with \tilde{x}_- being the stable equilibrium. It is worth noticing that the sympathetic oscillators correspond to the branch of the cubic parabola (23) corresponding to the x satisfying

$$\hat{x}_2(\mu) < x < 0 \quad \text{as } 0 < \mu < \mu_* \quad \text{and} \quad -\sqrt{1-\mu} < x < 0 \quad \text{as } \mu_* \leq \mu < 0.$$

The equilibrium existence region of the modified configuration (Figure 5, left, is depicted in Figure 5, right). The condition (28) is satisfied for two branches of the parabola (23) as $0 < \mu < \mu_*$, corresponding to the x satisfying

$$-\sqrt{1-\mu} \leq x \leq x_1(\mu) \quad \text{and} \quad x_2(\mu) \leq x \leq \hat{x}_2(\mu). \tag{30}$$

Also from the condition $x^* < x$, it follows that the first inequality of (30) specifies the modified model in the region A1 as $x^* < x_1(\mu)$, which is true if $\mu^* = 1/2\sqrt{2} < \mu$. Given $\mu = \mu_*$, these branches coalesce and as $\mu_* < \mu$ they specify the sole function $h(x, \mu)$ within the interval $(-\sqrt{1-\mu}, \hat{x}_2(\mu))$. The condition $-\sqrt{1-\mu} < \hat{x}_2(\mu)$ results in the inequality $\mu < \frac{1}{2}$. Therefore, the solution existence region is specified by

$$\begin{aligned} x_2(\mu) \leq x \leq \hat{x}_2(\mu) & \quad \text{as } 0 < \mu < \mu_*, \\ x^* \leq x < \hat{x}_2(\mu) & \quad \text{as } \mu_* \leq \mu < \frac{1}{2}, \\ x^* \leq x < x_1(\mu) & \quad \text{as } \mu^* \leq \mu < \mu_* \end{aligned}$$

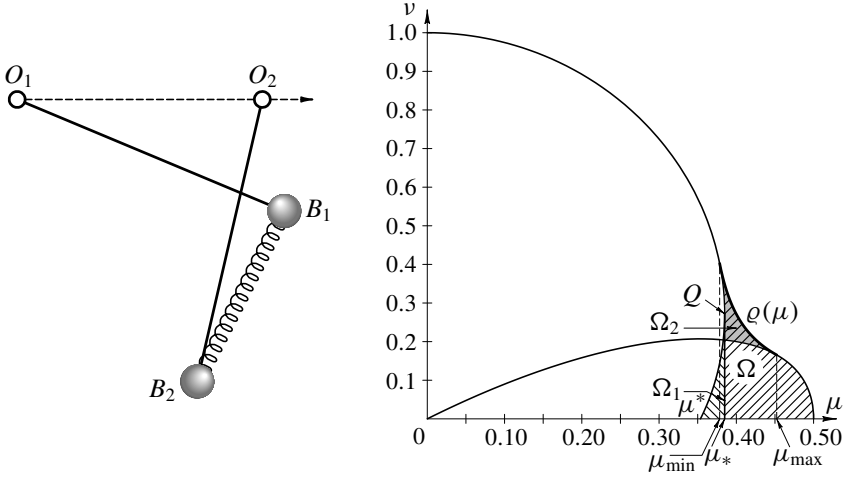


Figure 5. Left: the asymmetrical modified configuration in region A1. Right: the stability domain of the asymmetrical configuration is the merger of the regions Ω and Ω_1 .

and bounded by the curves $h(\hat{x}_2(\mu), \mu)$ and $h(-\sqrt{1-\mu}, \mu)$. Analogous to the case of the sympathetic oscillators, one can determine the boundary of the local maximum existence region for the function $h(x, \mu)$: $\mu_{\min} \approx 0.378424$ and $\mu_{\max} \approx 0.452258$.

The stability region Ω , corresponding to the branch of the cubic parabola with the point $x_2(\mu)$, encompasses the region Ω_2 of the two-equilibrium-solution existence. The stability region Ω_1 corresponds to the parabola's branch with the point $x_1(\mu)$. In the region of two-solution existence, there is a stable equilibrium corresponding to the solution \tilde{x}_- . The point Q indicates the coalescence point between the branches and equals $(2, \sqrt{2})/3\sqrt{3}$.

The region A2. In this case, we write (22) in the form

$$\mu \frac{s - \mu}{s} k(x) = -v. \quad (31)$$

The solutions of (31) exist if $-1 < x < x^*$. Since $x^* \leq \hat{x}_2(\mu)$ and $x^* \leq -\sqrt{1-\mu}$, the sympathetic oscillators have no asymmetric equilibria in the region A2.

The modified configurations exist if $s < \mu$ or $x < x^*$. This condition is satisfied if $-\sqrt{1-\mu} < x < x_1(\mu)$ as $0 < \mu < \mu^*$ and $-\sqrt{1-\mu} < x < x^*$ as $\mu^* \leq \mu < \frac{1}{2}$. Since $x < -\frac{1}{2}$ and $s < \mu$, the function $h(x, \mu)$ increases, i.e., $h'(x, \mu) > 0$. The solution existence region is specified by the inequalities $h(-\sqrt{1-\mu}, \mu) < v < h(x_1(\mu), \mu)$ as $0 < \mu < \mu^*$ and $h(-\sqrt{1-\mu}, \mu) < v < 0$ as $\mu^* \leq \mu < \frac{1}{2}$. Since $\det \Pi'' = v h'(x, \mu)/x$ and $x < 0$, then $\det \Pi'' < 0$ and there is no stable equilibrium in the region A2.

5. Conclusions

The analysis of the stability of two coupled oscillators showed that the model solutions significantly depend on the dimensionless parameters of varied physical origins. We demonstrated that the natural dimensionless kinematic parameter μ is subjected to the relation of the distance between the suspension points and the oscillator length. The dimensionless energetic parameter ν is equal to the relation between the potential energy of the oscillator and the spring's effective energy. Thus, the parameter set (μ, ν) presents the convenient variables of the model.

Though we considered a static case, dynamic stability of such systems was investigated using chains of particles connected by springs, some of which could exhibit negative stiffness [Pasternak et al. 2014]. The necessary stability condition was formulated: only one spring in the chain can have negative stiffness, and the value of negative stiffness cannot exceed a certain critical value. Applying the Cosserat theory with negative Cosserat shear modulus was proposed in [Pasternak et al. 2016]. It was shown that, when the sum of the negative Cosserat shear modulus and the conventional shear modulus is positive, the waves can propagate.

The demonstrated phenomena of the system's critical dynamics of the linked oscillators are important to general understanding of the nature of different processes. At macroscales, they play a crucial role in determining the fragility and instability of rocks [Tarasov and Guzev 2013] whereas at microscales the dynamics of phononic crystals that are lattices of linked oscillators is governed by the parameters (μ, ν) [Ghasemi Baboly et al. 2013]. In addition, an important application is magnetic tweezers, which may permit us to handle even single micromolecules [Lipfert et al. 2009].

References

- [Arkipova and Luongo 2014] I. M. Arkipova and A. Luongo, "Stabilization via parametric excitation of multi-dof statically unstable systems", *Commun. Nonlinear Sci. Numer. Simul.* **19**:10 (2014), 3913–3926.
- [Arkipova et al. 2012] I. M. Arkipova, A. Luongo, and A. P. Seyranian, "Vibrational stabilization of the upright statically unstable position of a double pendulum", *J. Sound Vib.* **331**:2 (2012), 457–469.
- [Butikov 2011] E. I. Butikov, "An improved criterion for Kapitza's pendulum stability", *J. Phys. A* **44**:29 (2011), 295202.
- [dell'Isola et al. 2016] F. dell'Isola, I. Giorgio, M. Pawlikowski, and N. L. Rizzi, "Large deformations of planar extensible beams and pantographic lattices: heuristic homogenization, experimental and numerical examples of equilibrium", *P. Roy. Soc. A* **472**:2185 (2016), 20150790.
- [Ghasemi Baboly et al. 2013] M. Ghasemi Baboly, M. F. Su, C. M. Reinke, S. Alaie, D. F. Goettler, I. El-Kady, and Z. C. Leseman, "The effect of stiffness and mass on coupled oscillations in a phononic crystal", *AIP Adv.* **3**:11 (2013), 112121.

- [Huynh and Chew 2010] H. N. Huynh and L. Y. Chew, “Two-coupled pendulum system: bifurcation, chaos and the potential landscape approach”, *Internat. J. Bifur. Chaos Appl. Sci. Engrg.* **20**:8 (2010), 2427–2442.
- [Huynh et al. 2013] H. N. Huynh, T. P. T. Nguyen, and L. Y. Chew, “Numerical simulation and geometrical analysis on the onset of chaos in a system of two coupled pendulums”, *Commun. Nonlinear Sci. Numer. Simul.* **18**:2 (2013), 291–307.
- [Kapitza 1951a] P. L. Kapitza, “Маятник с вибрирующим подвесом” (“Pendulum with vibrating suspension”), *Usp. Fiz. Nauk.* **44**:5 (1951), 7–20.
- [Kapitza 1951b] P. L. Kapitza, “Динамическая устойчивость маятника при колеблющейся точке подвеса”, *Zh. Eksp. Teor. Fiz.* **21**:5 (1951), 588–592. Translated as “Dynamical stability of a pendulum when its point of suspension vibrates” pp. 714–725 in *Collected papers of P. L. Kapitza*, vol. 2, edited by D. ter Haar, Pergamon, London, 1965.
- [Kittel 2005] C. Kittel, *Introduction to solid state physics*, 8th ed., Wiley, Hoboken, NJ, 2005.
- [Koluda et al. 2014] P. Koluda, P. Perlikowski, K. Czolczynski, and T. Kapitaniak, “Synchronization configurations of two coupled double pendula”, *Commun. Nonlinear Sci. Numer. Simul.* **19**:4 (2014), 977–990.
- [Lipfert et al. 2009] J. Lipfert, X. Hao, and N. H. Dekker, “Quantitative modeling and optimization of magnetic tweezers”, *Biophys. J.* **96**:12 (2009), 5040–5049.
- [Maianti et al. 2009] M. Maianti, S. Pagliara, G. Galimberti, and F. Parmigiani, “Mechanics of two pendulums coupled by a stressed spring”, *Am. J. Phys.* **77**:9 (2009), 834–838.
- [Markeev 2013] A. P. Markeev, “О движении связанных маятников” (“On the motion of connected pendulums”), *Nelin. Dinam.* **9**:1 (2013), 27–38.
- [Pasternak et al. 2014] E. Pasternak, A. V. Dyskin, and G. Sevel, “Chains of oscillators with negative stiffness elements”, *J. Sound. Vib.* **333**:24 (2014), 6676–6687.
- [Pasternak et al. 2016] E. Pasternak, A. V. Dyskin, and M. Esin, “Wave propagation in materials with negative Cosserat shear modulus”, *Int. J. Eng. Sci.* **100** (2016), 152–161.
- [Pikovsky and Rosenblum 2015] A. Pikovsky and M. Rosenblum, “Dynamics of globally coupled oscillators: progress and perspectives”, *Chaos* **25** (2015), 097616.
- [Ramachandran et al. 2011] P. Ramachandran, S. G. Krishna, and Y. M. Ram, “Instability of a constrained pendulum system”, *Am. J. Phys.* **79**:4 (2011), 395–400.
- [Seyranian and Seyranian 2008] A. A. Seyranian and A. P. Seyranian, “Chelomei’s problem of the stabilization of a statically unstable rod by means of a vibration”, *J. Appl. Math. Mech.* **72**:6 (2008), 649–652.
- [Sommerfeld 1994] A. Sommerfeld, *Vorlesungen über theoretische Physik*, Band I: Mechanik, Harri Deutsch, Thun, Switzerland, 1994.
- [Stephenson 1908] A. Stephenson, “On induced stability”, *Philos. Mag.* (6) **15**:86 (1908), 233–236.
- [Tarasov and Guzev 2013] B. G. Tarasov and M. A. Guzev, “Mathematical model of fan-head shear rupture mechanism”, *Key Eng. Mat.* **592–593** (2013), 121–124.

Received 8 Nov 2015. Revised 11 Apr 2016. Accepted 14 May 2016.

MICKHAIL A. GUZEV: guzev@iam.dvo.ru

Institute for Applied Mathematics, Far Eastern Branch, Russian Academy of Sciences, Radio 7, Vladivostok, 690041, Russia

ALEXANDR A. DMITRIEV: dmitriev@iam.dvo.ru

Institute for Applied Mathematics, Far Eastern Branch, Russian Academy of Sciences, Radio 7, Vladivostok, 690041, Russia



MATHEMATICS AND MECHANICS OF COMPLEX SYSTEMS

msp.org/memocs

EDITORIAL BOARD

ANTONIO CARCATERRA	Università di Roma "La Sapienza", Italia
ERIC A. CARLEN	Rutgers University, USA
FRANCESCO DELL'ISOLA	(CO-CHAIR) Università di Roma "La Sapienza", Italia
RAFFAELE ESPOSITO	(TREASURER) Università dell'Aquila, Italia
ALBERT FANNJIANG	University of California at Davis, USA
GILLES A. FRANCFORT	(CO-CHAIR) Université Paris-Nord, France
PIERANGELO MARCATI	Università dell'Aquila, Italy
JEAN-JACQUES MARIGO	École Polytechnique, France
PETER A. MARKOWICH	DAMTP Cambridge, UK, and University of Vienna, Austria
MARTIN OSTOJA-STARZEWSKI	(CHAIR MANAGING EDITOR) Univ. of Illinois at Urbana-Champaign, USA
PIERRE SEPPECHER	Université du Sud Toulon-Var, France
DAVID J. STEIGMANN	University of California at Berkeley, USA
PAUL STEINMANN	Universität Erlangen-Nürnberg, Germany
PIERRE M. SUQUET	LMA CNRS Marseille, France

MANAGING EDITORS

MICOL AMAR	Università di Roma "La Sapienza", Italia
CORRADO LATTANZIO	Università dell'Aquila, Italy
ANGELA MADEO	Université de Lyon-INSA (Institut National des Sciences Appliquées), France
MARTIN OSTOJA-STARZEWSKI	(CHAIR MANAGING EDITOR) Univ. of Illinois at Urbana-Champaign, USA

ADVISORY BOARD

ADNAN AKAY	Carnegie Mellon University, USA, and Bilkent University, Turkey
HOLM ALTENBACH	Otto-von-Guericke-Universität Magdeburg, Germany
MICOL AMAR	Università di Roma "La Sapienza", Italia
HARM ASKES	University of Sheffield, UK
TEODOR ATANACKOVIĆ	University of Novi Sad, Serbia
VICTOR BERDICHEVSKY	Wayne State University, USA
GUY BOUCHITTÉ	Université du Sud Toulon-Var, France
ANDREA BRAIDES	Università di Roma Tor Vergata, Italia
ROBERTO CAMASSA	University of North Carolina at Chapel Hill, USA
MAURO CARFORE	Università di Pavia, Italia
ERIC DARVE	Stanford University, USA
FELIX DARVE	Institut Polytechnique de Grenoble, France
ANNA DE MASI	Università dell'Aquila, Italia
GIANPIETRO DEL PIERO	Università di Ferrara and International Research Center MEMOCS, Italia
EMMANUELE DI BENEDETTO	Vanderbilt University, USA
BERNOLD FIEDLER	Freie Universität Berlin, Germany
IRENE M. GAMBA	University of Texas at Austin, USA
DAVID Y. GAO	Federation University and Australian National University, Australia
SERGEY GAVRILYUK	Université Aix-Marseille, France
TIMOTHY J. HEALEY	Cornell University, USA
DOMINIQUE JEULIN	École des Mines, France
ROGER E. KHAYAT	University of Western Ontario, Canada
CORRADO LATTANZIO	Università dell'Aquila, Italy
ROBERT P. LIPTON	Louisiana State University, USA
ANGELO LUONGO	Università dell'Aquila, Italia
ANGELA MADEO	Université de Lyon-INSA (Institut National des Sciences Appliquées), France
JUAN J. MANFREDI	University of Pittsburgh, USA
CARLO MARCHIORO	Università di Roma "La Sapienza", Italia
GÉRARD A. MAUGIN	Université Paris VI, France
ROBERTO NATALINI	Istituto per le Applicazioni del Calcolo "M. Picone", Italy
PATRIZIO NEFF	Universität Duisburg-Essen, Germany
ANDREY PIATNITSKI	Narvik University College, Norway, Russia
ERRICO PRESUTTI	Università di Roma Tor Vergata, Italy
MARIO PULVIRENTI	Università di Roma "La Sapienza", Italia
LUCIO RUSSO	Università di Roma "Tor Vergata", Italia
MIGUEL A. F. SANJUAN	Universidad Rey Juan Carlos, Madrid, Spain
PATRICK SELVADURAI	McGill University, Canada
ALEXANDER P. SEYRANIAN	Moscow State Lomonosov University, Russia
MIROSLAV ŠILHAVÝ	Academy of Sciences of the Czech Republic
GUIDO SWEERS	Universität zu Köln, Germany
ANTOINETTE TORDSILLAS	University of Melbourne, Australia
LEV TRUSKINOVSKY	École Polytechnique, France
JUAN J. L. VELÁZQUEZ	Bonn University, Germany
VINCENZO VESPRI	Università di Firenze, Italia
ANGELO VULPIANI	Università di Roma La Sapienza, Italia

MEMOCS (ISSN 2325-3444 electronic, 2326-7186 printed) is a journal of the International Research Center for the Mathematics and Mechanics of Complex Systems at the Università dell'Aquila, Italy.

Cover image: "Tangle" by © John Horigan; produced using the *Context Free* program (contextfreeart.org).

PUBLISHED BY



mathematical sciences publishers
nonprofit scientific publishing

<http://msp.org/>

© 2016 Mathematical Sciences Publishers

Constraint reaction and the Peach–Koehler force for dislocation networks	105
Riccardo Scala and Nicolas Van Goethem	
Stability analysis of two coupled oscillators	139
Mikhail A. Guzev and Alexandr A. Dmitriev	
Analysis of the electromagnetic reflection and transmission through a stratified lossy medium of an elliptically polarized plane wave	153
Fabio Mangini and Fabrizio Frezza	
Dislocation-induced linear-elastic strain dynamics by a Cahn–Hilliard-type equation	169
Nicolas Van Goethem	

MEMOCS is a journal of the International Research Center for the Mathematics and Mechanics of Complex Systems at the Università dell’Aquila, Italy.

